Tetrahedron Formation Control[1]

José J. Guzmán[2]

Abstract

This paper considers the preliminary development of a general optimization procedure for tetrahedron formation control. The maneuvers are assumed to be impulsive and a multi-stage optimization method is employed. The stages include (1) targeting to a fixed tetrahedron location and orientation, and (2) rotating and translating the tetrahedron. The number of impulsive maneuvers can also be varied. As the impulse locations and times change, new arcs are computed using a differential corrections scheme that varies the impulse magnitudes and directions. The result is a continuous trajectory with velocity discontinuities. The velocity discontinuities are then used to formulate the cost function. Direct optimization techniques are employed. The procedure is applied to the NASA Goddard Magnetospheric Multi-Scale (MMS) mission to compute preliminary formation control fuel requirements.

[1]A previous version was presented at the 2003 Flight Mechanics Symposium at NASA Goddard Space Flight Center.

[2]Aerospace Engineer, Mission Analysis Department

a.i. solutions, Inc., 10001 Derekwood Lane, Suite 215, Lanham, MD 20706, USA

Introduction

The purpose of this paper is to introduce and to motivate further study of some of the ideas and concepts needed to successfully fly the NASA Goddard Magnetospheric Multi-Scale mission. Specifically, this paper reports the results of a preliminary study on the development of a general optimization procedure for tetrahedron formation control. In general, for this type of in-situ mission, maintaining a tight formation during the orbital evolution is not necessary. It is of importance, however, to be able to change the tetrahedron size and to maintain shape metrics (quality factors [1]) within "acceptable" values during specific times. Typically, the quality factor maximization can be achieved by a judicious choice of initial conditions. The formation then evolves naturally (without maneuvers) while collecting science data. In this investigation, the maneuvers needed to transfer the formation from its current configuration to the initial conditions at the beginning of the science arc are examined. In an effort to minimize fuel expenditure, a multi-stage optimization method is employed. The algorithms developed for this investigation do not make any assumptions on the location and number of burns that will be used. Direct optimization techniques that have been presented and examined previously are used [2]. No claims are made about the global optimality of the solutions, only that the solutions computed are local optima given the inputs and constraints. In fact, an experienced analyst might be able to take some of the resulting solutions and further improve them via numerical experimentation. Nevertheless, the ultimate goal is to automate the mission design process as much as possible by quickly computing solutions that

are at least local minima. The methodology is applied to the MMS mission to gain understanding about the fuel needed to perform certain tasks.

Previous Work

Tetrahedron formations are excellent scientific platforms for magnetic field studies. A tetrahedron mission, Cluster II, is currently flying and operating successfully [3]. In the process of planning the Cluster mission, fuel optimization of the maneuvers needed to initialize, modify and maintain the formation was considered by Rodríguez-Canabal and Belló-Mora [4]. Later a different optimization method was employed by Schoenmaekers [5]. In Schoenmaekers's paper, both methods are compared for one mission scenario. Moreover, a further-developed strategy is presented by Belló-Mora and Rodríguez-Canabal [6]. Implementation and operational results for the maneuvers are reported by Hockens and Schoenmaekers [7]. These Cluster references provide a solid foundation for the work in the current investigation.

In this paper the mission of interest is the MMS Mission. MMS will determine the small-scale basic plasma processes which transport, accelerate and energize plasmas in thin boundary and current layers. These processes control the structure and dynamics of the Earth's magnetosphere [8]. For the interested reader, preliminary mission design and analysis for MMS, which includes a double lunar swingby for one of its phases, has been presented by: Edery and Schiff [9], Edery [10], Guzmán and Edery [11,12], Petruzzo [13], and Hughes [14,15].

Approach

For the purpose of this investigation the formation flying design is divided into two distinct arcs. The first arc includes a sequence of maneuvers that transfers the formation from its current configuration (position and velocity states) to a configuration appropriate for the start of the second arc, the science one. Denote the formation configuration at the beginning of the science arc as the target configuration. See Fig. . Note that the science arc does not contain any maneuvers. In fact, the absence of maneuvers benefits the science data gathering by limiting the orbital disturbances. The two arcs then lead to two coupled optimization problems: (i) compute the initial states of the science arc that maximize a certain tetrahedron quality factor along the science arc, and (ii) compute the maneuver sequence that minimizes the fuel needed to transfer the formation from its current configuration to the target configuration. In this paper, only the second problem is considered. In references [13, 14] the first problem is considered. Since the two problems are coupled, the goal is to eventually merge these two optimization processes. For now, a target configuration is assumed to develop algorithms that solve the second problem. In other words, the four states that comprise the target configuration are considered as given for the maneuver optimization process. Nonetheless, as a way of finding the greatest lower bound on fuel consumption, rotations and translations of the target tetrahedron have been allowed. Eventually, both quality factor and fuel consumption considerations will determine the target configuration.

The Concept of a Reference Path

The trajectory design strategy for MMS involves obtaining a reference or nominal path that traverses the magnetospheric regions of interest. Relative to this defined reference path, a tetrahedron formation is established at certain times (specified by the scientists) during the mission. The science mission consists of four phases: the first two phases traverse regions of the magnetosphere close to the magnetic equatorial plane, the third phase contains a double lunar swingby sequence (**DLS**) with an investigation of the deep tail magnetospheric region, and the fourth phase explores regions perpendicular to the ecliptic. The different MMS phases and their corresponding scientific goals are explained by Curtis [8]. The science goals, in turn, help to specify the orbital requirements for each phase. The main orbital requirements are shown in Table (where $R_\oplus$ is the mean Earth radius). It is likely that some flexibility in the location of the formation relative to the reference path might be allowed (if the magnetospheric regions of interest are still traversed by the formation). Furthermore, the reference trajectory could be redefined. Still, since one of the phases includes a double lunar swingby, monitoring the formation relative to the reference path is of interest.[3]

Coordinate Systems

For the purpose of this investigation, three orthogonal Cartesian coordinate systems are employed. The first system is the geocentric inertial (**GCI**) frame. The inertial

[3]Because the reference path has been designed with the proper phasing for the lunar encounters.

frame is defined using the mean equatorial plane and the mean vernal equinox at Julian year 2000. The second frame utilizes the reference path orbital velocity, binormal and normal directions (**VBN**). The third frame is introduced to consider tetrahedron translation and rotations. It is placed at the tetrahedron centroid and it is initially coincident with the second frame. See Fig. . Table summarizes the frames employed (and their respective origins) and introduces the unit vector notation used in Fig. .

Initial Conditions for the Science Arc

The algorithms developed for this study are independent of the initial states selected for the science arc; yet the actual computations depend on them. Thus, in this section, an approximation to select the targets states at the beginning of the science arc is explained (other choices are possible). A regular tetrahedron[4] is used to meet the science data collection requirements. A reference orbit is specified and the individual spacecraft locations (position components) are set using spherical coordinates in the VBN frame [17].

The velocity directions are kept the same as that of the reference orbit, that is, the VBN frame velocity direction. This assumption is adequate when the spacecraft-to-reference separation is "small" relative to the reference-to-Earth separation (it should be revisited for large separations). Nonetheless, changing the velocity directions can be utilized to maximize a certain tetrahedron quality factor. This quality factor optimization has been investigated by Petruzzo [13]. The investigation has been extended

[4]A regular tetrahedron is useful in cases where sampling of the structure of a field is not as important as understanding its transient or fluctuating events [16].

by Hughes [14] to consider both the initial positions (non-regular tetrahedrons) and velocities.

The velocity magnitude is obtained using the two-body problem energy or vis-viva equation: $v = \sqrt{\mu\,(2/r - 1/a)}$, where v is the velocity magnitude, r is the position magnitude (radial distance), μ is the gravitational parameter and a is the semi-major axis. For orbital periodicity, the reference semi-major axis is utilized for all the spacecraft.

Initial Guess for the Maneuver Sequence

The first step in optimizing a particular problem is to obtain an initial guess. In this case an initial guess is obtained by propagating from some initial configuration. The initial states for the maneuver arc are also specified as explained in the *Initial Conditions for the Science Arc* section. (This specification is for computational convenience. During spacecraft operations the states would be set by the formation configuration at the specified start time for the maneuver arc). Then, the reference and the four spacecraft formation are propagated without any maneuvers. While propagating, discrete states along the path are saved. The discretization interval is selected by the user. In this case, a discretization in terms of true anomaly (**TA**) along the reference path is utilized. See Fig. for true anomaly discretizations of 180, 90, 45 and 22.5 degrees. These discretizations provide 3, 5, 9, and 17 "patch states" respectively. These patch states are discrete states where maneuvers might be implemented. Other anomalies (e.g. mean or eccentric) could be used for the discretization.[5] Now, it is

[5]In fact, the resulting optimal maneuver patterns should be compared in future studies.

important to realize that a spacecraft path with, for instance, 17 maneuvers is hard to implement in practice (operationally). Nevertheless, numerically implementing such a path will show the best locations to perform the maneuvers. Furthermore, many of the resulting maneuvers are "small" and can be eliminated and/or combined. As a result, the mission analyst can compute operationally feasible solutions.

Computing the Optimal Maneuver Sequence

Once the initial and final states have been set for the maneuver sequence, the target/optimization process can proceed. The optimization approach involves combining the fuel optimization of each spacecraft with the minimization of the total fuel usage to achieve a target configuration. The total fuel usage is the sum of the totals for each of the four spacecraft (**S/C**). In terms of the spacecraft engine, only impulsive maneuvers are considered (thus only velocity change or $\mathbf{\Delta V}$ numbers are presented). For computational speed purposes, the optimization is performed sequentially (separately) in two stages: (1) each spacecraft trajectory is optimized by minimizing the fuel used by each spacecraft to achieve its target location in the tetrahedron, then, (2) the final tetrahedron configuration is varied (translated and rotated relative to some arbitrary configuration in the vicinity of the reference path) while minimizing the sum of all the spacecraft ΔVs. Better results might be obtained by completely embedding step (1) in each iteration of step (2) or by performing step (2) first and then step (1). Nevertheless, if the target orientation is specified by the scientific requirements and/or by the optimization of a certain quality factor, step (2) might not be allowed.

For both stages, as the impulse locations and times change (i.e., as the initial patch states in Fig. change), new arcs are computed using a differential corrections scheme that varies the impulse magnitudes and directions. See reference [2] for more details.

In the first optimization stage and for each spacecraft, the transfer trajectory problem becomes essentially a rendezvous problem. Specifically, each spacecraft path is discretized into a set of n patch states. The independent variables chosen are the changes in the internal and final patch state locations and times (i.e., four independent variables at each patch state). Thus, there are $4 \times (n-1)$ independent variables per spacecraft. For numerical purposes, the changes are constrained to stay within some user defined limits. Moreover, less flexibility is allowed in the final states (position and time are constrained to be within 10% of the desired inter-spacecraft distance and within 0.5 seconds of the desired final time respectively). Each spacecraft trajectory is optimized independently using the total ΔV as the cost function. The optimization method selected is the Sequential Quadratic Programming (SQP) method. This direct method is employed due to its efficiency in solving a large variety of cases. (See Ref. [2] for a comparison of different methods).

In the second optimization stage, the target tetrahedron is allowed to translate within some limits and to rotate about its initial centroid. The sum of all the spacecraft ΔVs is the cost function. The optimization method selected for the second stage is a Genetic Algorithm (GA) that varies 6 independent variables (3 variables for the translation and 3 variables for the rotation). Although other choices are possible, this stochastic method is selected to avoid local minima and, most importantly, to prepare for augmenting the cost function with science and operational constraints (the aug-

mentation might result in discontinuities in the cost function). For this preliminary investigation, following some empirically developed guidelines [18], a population size of $N = 4b$, where b is the number of bits in the binary chromosome, and a mutation probability of $P_{\text{mut}} = (b+1)/2Nb$ were utilized. These and other details of the setup for the GA are still under investigation.

Some Results for MMS

The methodology described in this paper is applied to the MMS mission. The reference orbital states considered are consistent with the orbit requirements of MMS (see Table). Now, although the algorithms developed for this study are independent of the particulars of the force model and integrator, the actual computations depend on them. Thus, the dynamical model that is adopted to represent the forces on the spacecraft includes the gravitational influences of the Sun, Earth and Moon (all obtained from the Jet Propulsion Laboratory Definitive Ephemeris 405 file). Solar radiation pressure (flat plate model) and the Earth's J_2 Earth gravity harmonic are also included. For the numerical integration scheme, a Runge-Kutta-Verner 8(9) integrator is utilized. Next, some results and discussion are presented for each mission phase.

Phases 1 and 2

As a test, different cases (with 3, 5, 9, and 17 maneuvers per spacecraft) are examined *for one orbit revolution.* That is, the initial states are specified at the apogee of the

reference orbit and the target states are at the next apogee.[6] Then, for both phases, three initial and three final tetrahedron sizes (inter-spacecraft separations between each spacecraft) are considered: 10, 1000, and 2000 km. These separations are consistent with preliminary science specifications [8]. For each initial separation, three target separations are considered while keeping the pre-maneuver (initial) conditions the same. Therefore, when the initial and target sizes are the same, the problem is a formation maintenance problem; otherwise, it is a re-sizing problem. Recall that the reference orbital requirements are shown in Table . For now, Phase 2 is assumed to have a 10 degree equatorial inclination.

The results for Phase 1 are in Table and the results for Phase 2 are in Table . The majority of the cost function values associated with Phase 1 are higher than for Phase 2. Therefore, a more extensive analysis should be performed to understand the perturbation effects (e.g. Earth's J_2, luni-solar perturbations and solar radiation pressure) on the tetrahedron evolution during the different orbital phases. Another interesting aspect is that the ΔV expenditure between the four spacecraft exhibits large differences in some of the cases. This particular problem can be remedied by adding constraints that require that the total ΔV of each spacecraft be within some (user defined) range relative to the total ΔV of any other spacecraft.

While computing some of these test cases, it was observed that the tetrahedron translation and rotations did not help to lower the total ΔV in the one-orbit revolution maintenance cases. This fact is not surprising given the fact that only one

[6] At the moment, regions near apogee are of interest to the scientists. However, other regions could be considered later on.

revolution was considered and the perturbation effects did not cause the formation to deviate significantly. Nonetheless, during actual mission operations, more than one orbit revolution will most likely elapse before tetrahedron maintenance is required. The actual maintenance schedule will depend, among other things, on how much degradation of the quality factors can be tolerated while still being able to perform "effective" science data collection.

It is also observed that re-sizing cases such as a 10 to 1000 km and 1000 to 10 km have similar costs. It is important to understand that these cases are not the same. That is, a tetrahedron with inter-spacecraft separation of 10 km and propagated for one orbit revolution undergoes different orbital perturbations than one with a 1000 km separation. Again, a more detailed perturbation analysis should be performed. Note that some cases did not "converge". This label means that either the differential corrector could not meet the requested tolerance or that the ΔV computed exceeded some user defined limit. In Tables and the cases that did not "converge" are all three-impulse re-sizing cases that exceeded the user defined ΔV limit. For these non-convergent cases, the initial angle between any two impulses is 180 degrees with the actual locations being at the apses. As a result, the differential corrector (which utilizes the orbit state transition matrix) encounters a singularity [19]. Specifically, after some iterations the fourth spacecraft has a significantly different orbit plane relative to the other spacecraft (after the second impulse at perigee). Fortunately, this particular problem has physical meaning and constraining the transfer plane can remedy the situation. Future work should correct these and other non-convergent cases and improve the automation process.

Phase 3

In Phase 3, the formation will traverse the deep tail of the magnetosphere during a double lunar swingby sequence [11]. At this point, there is no plan to perform any deterministic maneuvers for formation flying. That is, the final maneuver at perigee before the first lunar swingby produces a trajectory that requires no further maneuvers until Phase 4 begins after the second swingby. Thus, the formation will evolve under its natural dynamics in the perturbed Sun-Earth-Moon system. Non-deterministic maneuvers, however, will be used for any needed corrections.

Phase 4

Next, after the double lunar swingby sequence, it is of interest to know how much fuel would be required to restore the tetrahedron at the next apogee. In reference [11], three maneuvers (after the double lunar swingby) were used to restore the tetrahedron at the target apogee: the maneuver at perigee (TA = 0 degrees), an additional maneuver at the semi-latus rectum radial distance (TA = 90 degrees), and a maneuver at the target apogee (TA = 180 degrees). The lowest ΔV cost computed was for an initial separation of 10 km at the beginning of Phase 3 and a target separation of 200 km at the apogee after the double lunar swingby. The ΔV results in reference [11] were high because each spacecraft was incorrectly constrained to be at its own apogee at the end of the sequence. In this investigation, only the reference spacecraft is at its apogee at the target time. Also, the maneuver locations and times can now change. See Table for the results. It should be remarked that this table is different from the

previous tables for Phases 1 and 2. Specifically, the formation was initialized before the DLS. Therefore, the start of the maneuver sequence is at the perigee *after* the DLS. At this perigee, the formation is not in a regular tetrahedron but in some elongated shape with an average inter-spacecraft distance of 24 km. Also, the formation traverses only half of the reference orbit.

Further Fuel Cost Reduction

Further reduction in the fuel cost might be obtained in some cases by running the optimization stages completely nested. That is, for each new target orientation compute the optimal trajectories for each spacecraft. This process requires more computational resources but can be done with selected cases. Other resources include, but are not limited to: (a) varying the final (target) time, (b) establishing the tetrahedron relative to one of the four spacecraft (thus, one spacecraft is not required to maneuver), and (c) allowing several orbit revolutions before performing any maneuvers (e.g. maintenance). In option (b), the analyst should check that deviations from the desired reference path do not have adverse science and trajectory effects.

Additional insight is obtained by looking at the required configuration changes in terms of the orbital elements. This insight might lead the analyst to lower cost solutions. In fact, by computing the orbital elements, it can be shown that formation re-sizings require mostly line of nodes and line of apsides changes. Therefore, the analysis by Lawden is relevant [20]. Furthermore, for MMS, it has also been observed that Lawden's primer vector theory (see reference [21] for example) provides better

initial guesses for the strategy examined in this paper. As a result, the primer vector approach is also currently under investigation [22].

Summary

The purpose of this paper is to introduce and to motivate further study of some of the ideas and concepts needed to successfully fly the NASA Goddard Magnetospheric Multi-Scale mission. Specifically, the problem of maneuvering a tetrahedron formation while minimizing fuel expenditure is considered. The optimization is successfully performed sequentially in two stages: (1) each spacecraft trajectory is optimized by minimizing the fuel used by each spacecraft to achieve its target location in the tetrahedron, and (2) the final tetrahedron configuration is varied (translated and rotated relative to some arbitrary configuration in the vicinity of the reference path) while minimizing the sum of all the spacecraft ΔVs. The methodology is applied to the MMS mission to gain understanding about the fuel needed to perform certain tasks. The ultimate goal is to automate the mission design process as much as possible by quickly computing solutions that are at least local minima. Future work includes the simultaneous optimization of the maneuver and science arcs, the application of the methodology to different mission scenarios, the inclusion of operational considerations/constraints and the integration of the developed software into the NASA Goddard mission analysis tools.

Acknowledgments

This work has been supported by the Flight Dynamics Analysis Branch (Guidance, Navigation and Control Division) at NASA Goddard Space Flight Center under contract NAS5-01090. The author would like to thank the task managers: Mr. C. Petruzzo from NASA Goddard and Mr. J. Dibble from a.i. solutions. Also, the author would like to thank Mr. S. Hughes from NASA Goddard and Dr. A. Edery, Ms. L. Mailhe and Mr. C. Schiff (all from a.i. solutions) for invaluable discussions on the topic.

References

[1] J. Guzmán and C. Schiff, "A Preliminary Study for a Tetrahedron Formation: Quality Factors and Visualization," *AIAA/AAS Astrodynamics Specialists Conference*, Monterey, California, August 4-8 2002. AIAA 02-4637.

[2] S. Hughes, L. Mailhe, and J. Guzmán, "A Comparison of Trajectory Optimization Methods for the Impulsive Minimum Fuel Rendezvous Problem," *26th Annual AAS Guidance and Control Conference*, Breckenridge, Colorado, February 5-9 2003. AAS 03-006.

[3] R. Mugellesi-Dow, J. Dow, and G. Gienger, "Cluster II: From Launch to First Constellation," *16th International Symposium on Space Flight Dynamics*, Pasadena, California, December 2001.

[4] J. Rodríguez-Canabal and M. Belló-Mora, "Cluster: Consolidated Report on Mission Analysis," European Space Operation Centre, Technical Report, Darmstadt, Germany, July 1990. ESOC CL-ESC-RP-0001.

[5] J. Schoenmaekers, "Cluster: Fuel Optimum Spacecraft Formation Control," *ESA Symposium on Space Flight Dynamics*, Darmstadt, Germany, pp. 419–425, European Space Agency, December 1991. SP-326.

[6] M. Belló-Mora and J. Rodríguez-Canabal, "On the 3-d Configurations of the Cluster Mission," *ESA Symposium on Space Flight Dynamics*, Darmstadt, Germany, pp. 471–479, European Space Agency, December 1991. SP-326.

[7] D. Hocken and J. Schoenmaekers, "Optimization of Cluster Constellation Manoeuvres," *16th International Symposium on Space Flight Dynamics*, Pasadena, California, December 2001.

[8] S. Curtis, "The Magnetospheric Multiscale Mission...Resolving Fundamental Processes in Space Plasmas," NASA Goddard Space Flight Center, Greenbelt, Maryland, December 1999. NASA/TM—2000-209883.

[9] A. Edery and C. Schiff, "The Double Lunar Swingby of the MMS Mission," *16th International Symposium on Space Flight Dynamics*, Pasadena, California, December 2001.

[10] A. Edery, "Designing Phase 2 for the Double-Lunar Swingby of the Magnetospheric Multiscale Mission (MMS)," *13th Space Flight Mechanics Meeting*, Ponce, Puerto Rico, February 9-13 2003. AAS 03-245.

[11] J. Guzmán and A. Edery, "Flying a Four-Spacecraft Formation by the Moon...Twice," *13th Space Flight Mechanics Meeting*, Ponce, Puerto Rico, February 9-13 2003. AAS 03-132.

[12] J. Guzmán and A. Edery, "Mission Design for the MMS Tetrahedron Formation," *2004 IEEE Aerospace Conference*, Big Sky, Montana, March 6-13 2004. Paper 1424.

[13] S. Curtis, C. Petruzzo, P. Clark, and A. Peterson, "The Magnetospheric Multi-Scale Mission: An Electronically Tethered Constellation of Four Spacecraft,"

3rd International Workshop on Satellite Constellations and Formation Flying, Pisa, Italy, International Astronautical Federation, February 24-26 2003.

[14] S. Hughes, "Formation Tetrahedron Design for Phase 1 of the Magnetospheric Multi-Scale Mission," *GSFC Flight Mechanics Symposium*, Greenbelt, Maryland, NASA Goddard Space Flight Center, October 28-30 2003.

[15] S. Hughes, "Orbit Design for Phase I and II of the Magnetospheric Multiscale Mission," *27th Annual AAS Guidance and Control Conference*, Breckenridge, Colorado, American Astronautical Society, February 4-8 2004. AAS 04-024.

[16] P. Robert, A. Roux, C. Harvey, M. Dunlop, P. Daly, and K. Glassmeier, "Tetrahedron Geometric Factors," *Analysis Methods for Multi-Spacecraft Data* (G. Paschmann and P. Daly, eds.), pp. 323–348, Noordwijk, The Netherlands: ISSI Report SR-001, ESA Publications Division, 1998.

[17] C. Schiff, D. Rohrbaugh, and J. Bristow, "Formation Flying in Elliptical Orbits," *2000 IEEE Aerospace Conference*, Big Sky, Montana, April 18-25 2000. Paper 317.

[18] E. Williams and W. Crossley, "Empirically-Derived Population Size and Mutation Rate Guidelines for a Genetic Algorithm with Uniform Crossover," *Soft Computing in Engineering Design and Manufacturing* (P. Chawdhry, R. Roy, and R. Pant, eds.), pp. 163–172, Springer-Verlag, 1998.

[19] R. Stern, "Singularities in the Analytic Solution of the Linearized Variational Equations of Elliptical Motion," Experimental Astronomy Lab., Massachusetts

Institute of Technology, Technical Report, Cambridge, Massachusetts, May 1964. Report RE-8.

[20] D. F. Lawden, *Impulsive Transfer Between Elliptic Orbits*, pp. 323–351. Optimization Techniques, New York: Academy Press, 1962. edited by G. Leitman.

[21] J. Guzmán, L. Mailhe, C. Schiff, S. Hughes, and D. Folta, "Primer Vector Optimization: Survey of Theory, New Analysis and Applications," *53rd International Astronautical Congress*, Houston, Texas, October 2002. IAC-02-A.6.09.

[22] L. Mailhe and J. Guzmán, "Initialization and Resizing of Formation Flying Using Global and Local Optimization Methods," *2004 IEEE Aerospace Conference*, Big Sky, Montana, March 6-13 2004. Paper 1425.

Figure Captions

Fig. 1: Maneuver and Science Arcs

Fig. 2: MMS Frames

Fig. 3: True Anomaly Discretization: Initial Maneuver Locations

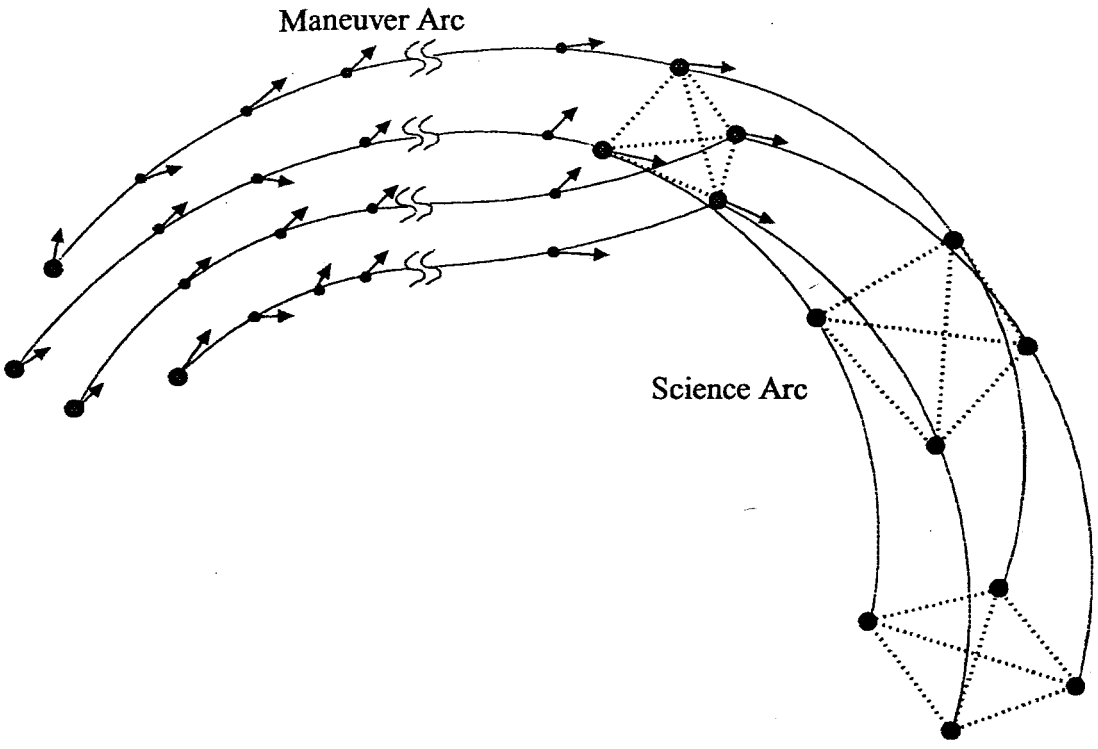
Maneuver Arc
Science Arc

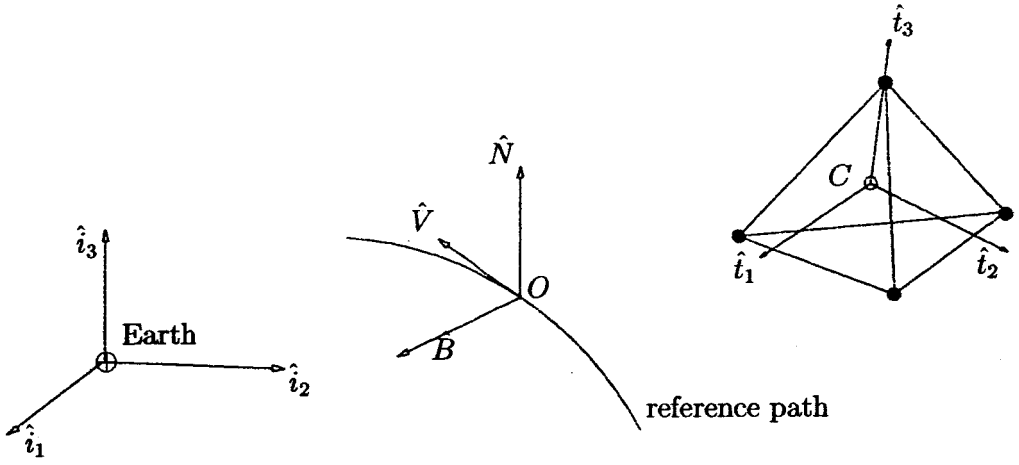
$\hat{t}_3$
$\hat{N}$
C
$\hat{V}$
$\hat{i}_3$
O
$\hat{t}_1$
$\hat{t}_2$
Earth
$\hat{B}$
$\hat{i}_2$
reference path
$\hat{i}_1$

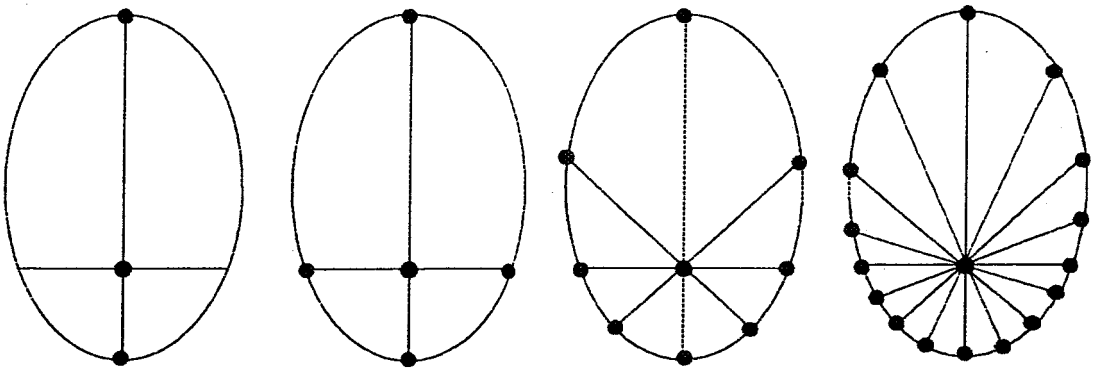

Table Captions

Table 1: MMS Orbital Requirements

Table 2: Coordinate Frames

Table 3: ΔV Cost as a Function of Initial and Final Separations in Phase 1

Table 4: ΔV Cost as a Function of Initial and Final Separations in Phase 2

Table 5: ΔV Cost for Restoring the Tetrahedron in Phase 4

Mission Phase	Perigee ($R_\oplus$)	Apogee ($R_\oplus$)	Semi-Major Axis ($R_\oplus$)	Eccentricity	Inclination (degrees)
Phase 0	1.2	12	6.6	0.818	$28.5 \rightarrow 10$ *
Phase 1	1.2	12	6.6	0.818	10*
Phase 2	1.2	30	15.6	0.923	10-20*
Phase 3	NA#	> 100	NA	NA	NA
Phase 4	10	40	25	0.600	~ 90**

Not Applicable, * Equatorial Inclination, ** Ecliptic Inclination

Type	Unit Vectors	Origin
Inertial	$(\hat{i}_1, \hat{i}_2, \hat{i}_3)$	$\oplus$ - Earth's center
Rotating	$(\hat{V}, \hat{B}, \hat{N})$	O - Reference spacecraft (fictitious)
Rotating	$(\hat{t}_1, \hat{t}_2, \hat{t}_3)$	C - Tetrahedron centroid

Impulses per S/C	ΔV_{SC1}	ΔV_{SC2}	ΔV_{SC3}	ΔV_{SC4}	ΔV_{TOTAL} [m/s]
10 to 10 km					
3	0.253	0.235	0.077	0.187	0.752
5	**0.028**	**0.023**	**0.010**	**0.022**	**0.084**
9	0.029	0.029	0.031	0.026	0.115
17	0.042	0.036	0.046	0.032	0.156
10 to 1000 km					
3	41.117	58.301	66.300	*	N/A
5	39.042	52.567	59.247	56.586	207.442
9	**42.195**	**47.223**	**60.079**	**32.298**	**181.795**
17	67.829	47.910	39.409	68.365	223.512
10 to 2000 km					
3	82.772	116.749	132.839	*	N/A
5	69.385	120.594	93.236	126.301	409.516
9	**77.264**	**61.698**	**148.880**	**74.064**	**361.906**
17	78.616	146.109	144.089	74.454	443.269
1000 to 10 km					
3	39.749	58.320	69.079	*	N/A
5	38.584	52.718	59.994	56.589	207.885
9	**35.835**	**50.819**	**58.251**	**44.049**	**188.954**
17	39.184	62.433	69.373	60.850	231.840
1000 to 1000 km					
3	0.508	0.592	1.275	0.081	2.457
5	**0.420**	**0.554**	**1.231**	**0.088**	**2.293**
9	0.415	0.563	1.219	0.102	2.299
17	0.616	0.754	1.706	0.114	3.189
1000 to 2000 km					
3	41.205	55.613	66.832	*	N/A
5	39.723	51.590	59.229	57.785	208.327
9	**36.540**	**49.710**	**58.098**	**44.388**	**188.736**
17	40.016	61.444	68.990	61.490	231.939
2000 to 10 km					
3	78.732	115.462	144.820	*	N/A
5	77.412	104.583	121.030	114.301	417.326
9	**71.936**	**101.521**	**118.155**	**88.540**	**380.153**
17	78.758	125.638	139.962	122.593	466.950
2000 to 1000 km					
3	38.559	45.998	71.591	*	N/A
5	38.514	52.814	62.622	57.765	211.715
9	**35.859**	**51.287**	**60.888**	**44.602**	**192.637**
17	39.317	63.586	71.842	61.705	236.450
2000 to 2000 km					
3	0.914	1.097	3.186	0.154	5.351
5	0.814	1.078	2.870	0.173	4.936
9	**0.772**	**1.074**	**2.829**	**0.179**	**4.853**
17	1.149	1.433	3.955	0.189	6.726

* did not converge

Impulses per S/C	ΔV_{SC1}	ΔV_{SC2}	ΔV_{SC3}	ΔV_{SC4}	ΔV_{TOTAL} [m/s]
10 to 10 km					
3	0.076	0.043	0.011	0.024	0.153
5	**0.025**	**0.022**	**0.022**	**0.023**	**0.092**
9	0.026	0.027	0.028	0.025	0.105
17	0.037	0.037	0.040	0.037	0.151
10 to 1000 km					
3	17.491	23.479	23.479	*	N/A
5	15.203	19.530	20.617	21.954	77.304
9	12.794	15.701	19.958	8.847	57.300
17	**24.324**	**9.329**	**10.069**	**13.354**	**57.077**
10 to 2000 km					
3	35.130	46.833	46.612	*	N/A
5	45.762	44.764	32.428	28.986	151.940
9	**21.847**	**23.541**	**52.335**	**16.014**	**113.738**
17	21.790	44.021	16.849	31.597	114.257
1000 to 10 km					
3	17.165	23.630	27.834	*	N/A
5	14.823	19.980	21.078	22.037	77.918
9	12.349	16.424	19.565	12.669	61.008
17	**11.149**	**16.599**	**20.483**	**12.704**	**60.936**
1000 to 1000 km					
3	0.496	1.018	1.139	0.308	2.962
5	0.453	0.432	0.989	0.250	2.124
9	0.302	0.337	0.707	0.216	1.563
17	**0.274**	**0.340**	**0.688**	**0.216**	**1.518**
1000 to 2000 km					
3	18.440	22.728	23.067	*	N/A
5	15.613	19.066	20.522	22.293	77.494
9	**12.783**	**15.889**	**19.450**	**12.596**	**60.718**
17	16.976	17.150	16.283	22.126	72.534
2000 to 10 km					
3	78.732	115.462	144.820	*	N/A
5	30.032	39.156	43.167	44.310	156.664
9	24.644	32.582	40.185	25.438	122.848
17	**22.281**	**33.145**	**41.822**	**25.498**	**122.745**
2000 to 1000 km					
3	14.441	37.554	42.702	*	N/A
5	14.772	19.935	22.848	22.391	79.945
9	12.192	16.666	20.923	12.902	62.682
17	**11.007**	**16.854**	**21.711**	**12.933**	**62.505**
2000 to 2000 km					
3	1.003	1.265	3.331	0.655	6.253
5	0.867	0.803	2.274	0.482	4.426
9	0.563	0.621	1.607	0.407	3.198
17	**0.492**	**0.612**	**1.575**	**0.395**	**3.073**

* did not converge

Impulses per S/C	ΔV_{SC1}	ΔV_{SC2}	ΔV_{SC3}	ΔV_{SC4}	ΔV_{TOTAL} [m/s]
24 (avg.) to 200 km					
3	1.260	0.393	0.866	1.104	3.623
5	**1.078**	**0.812**	**1.107**	**0.532**	**3.530**
9	1.141	1.083	1.358	1.584	5.166
24 (avg.) to 1000 km					
3	**3.599**	**4.309**	**4.985**	**4.907**	**17.799**
5	3.824	4.862	5.330	4.911	18.927
9	7.564	7.948	6.287	5.777	27.577
24 (avg.) to 2000 km					
3	**6.343**	**10.917**	**10.537**	**9.307**	**37.104**
5	14.135	5.406	8.666	10.860	39.066
9	13.731	12.688	19.284	12.388	58.092